TECHNICAL DOCUMENT

Cradle CFD

This technical study presents a store separation validation simulation performed using MSC Cradle CFD software, in which the transient analysis results are compared with experimental test data.

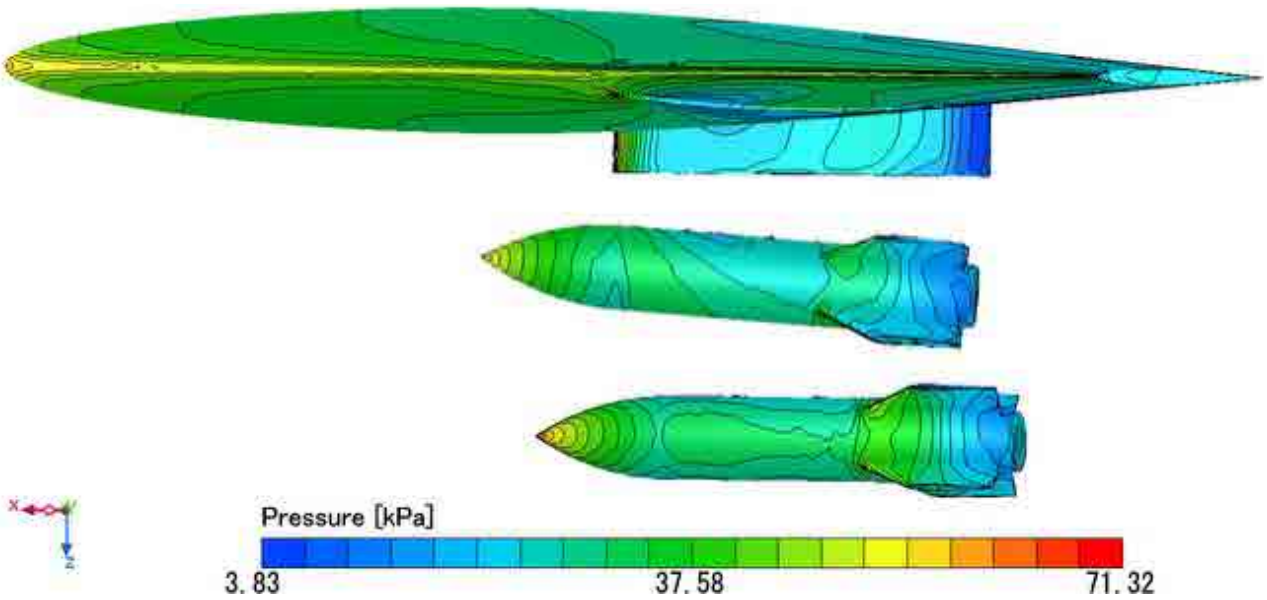

BİAS MÜHENDİSLİK

HEXAGON

Validation of Store Separation Using Cradle CFD with Experimental Data

Prepared by
Önder YILMAZ Senior Expert CFD Application Engineer

Date: 25/09/2025

During World War I, pilots manually dropped bombs from aircraft by hand. With advancing technology, bombs are now released from aircraft using specialized ejector mechanisms under the safest and most optimal conditions. Similarly, in spacecraft, depleted fuel tanks and mission-completed capsule stages are separated from the spacecraft using dedicated release systems. The release and separation of fuel tanks, munitions or payloads from aircraft play a critical role in overall mission safety. Two primary factors govern safe separation; the ejector mechanism and the aerodynamic configuration of the object. These factors determine the trajectory of the separated body. Until the 1960s, store separation tests could only be conducted through flight experiments, which were hazardous, costly and time-consuming. From the 1960s onward, wind tunnel testing began to be employed [1]. In these tests, scaled models of the aircraft are subjected to simulated environmental conditions. With further technological progress, Computational Fluid Dynamics (CFD) software started to be utilized for store separation analyses in the 1990s. Compared to flight and wind tunnel tests, CFD provides a significantly faster and more cost-effective alternative. Cradle CFD software, with its Overset Mesh method and 6DOF (6 degrees of freedom) rigid body solver, offers an effective approach for store separation analyses. In this technical paper, store separation analysis is conducted using Cradle CFD. The analysis results show good agreement with reference articles and experimental data [2].

1. INTRODUCTION

In this study, the Wing/Pylon/Finned store test model, which was tested in wind tunnel experiments conducted by the Arnold Engineering Development Center in 1991, was used as the reference model [2]. The tests were carried out using a 1/20 scale model and data were collected regarding the store's trajectory, aerodynamic forces, aerodynamic moments and surface pressure distribution. The wind tunnel test report presents the displacement of the finned store’s center of gravity along the X, Y, and Z axes, its linear velocity and its angular position values, recorded over 0.35 s [2].

2. STORE SEPARATION VALIDATION SIMULATION MODELING

The store separation validation study was carried out by constructing a three-dimensional model based on the geometric data provided in the reference paper. The mass properties of the finned store were implemented as boundary conditions in the simulation. In the initial phase, a steady state analysis was performed to allow the flow field around the geometry to develop and converge. The results of this steady state solution were then used as the initial condition for the transient analysis. During the transient simulation, the trajectory coordinates of the finned store were recorded over a time period of 0.35 seconds.

2.1 Test Model Used in Wind Tunnel Experiments

The images of the 1/20 scale model geometry used in the wind tunnel tests, as published in the report by the Arnold Engineering Development Center, are presented in Figure 1 [3].

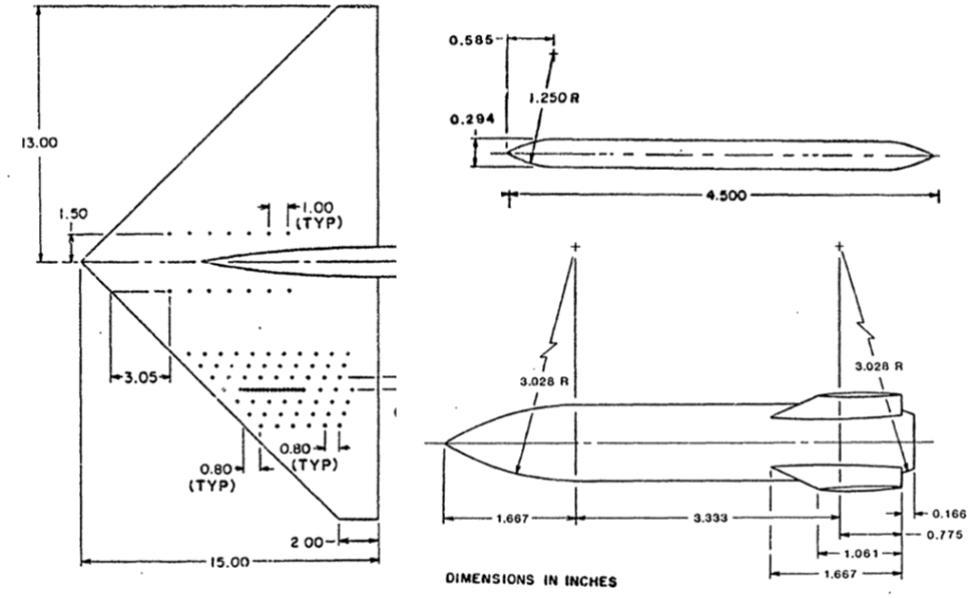

Figure 1: Detailed geometric specifications of the 1/20 scale wind tunnel test model

The wing geometry used in the wind tunnel tests features a NACA-64A010 airfoil cross section. The leading-edge sweep angle of the wing is 45°. The root chord length is 7.62 m, while the tip chord length is 1.016 m. The store geometry has a cylindrical body with a diameter of 0.508 m. The store's nose cone is of an ogive shape, with an ogive radius of 1.538 m and a distance of 0.846 m from the ogive radius center to the nose cone tip. Similarly, the aft cone has an ogive radius of 1.538 m, with a distance of 0.478 m from the radius center to the rear edge. The total length of the store is 3.018 m. The center of gravity of the finned store is located 1.416 m from the tip of the nose cone. The finned store is equipped with four fins, each having a NACA-0008 airfoil profile. The fins have a leading-edge sweep angle of 60°, a height of 0.223 m and a tip chord length of 0.538 m. The pylon geometry consists of a flat plate cross section with a width of 0.149 m. The leading and trailing edges of the pylon have an ogive shape, with an ogive radius of 0.635 m and a distance of 0.297 m to the tip. Using the geometric

data provided in the test report, a 3D model of the Wing/Pylon/Finned store was constructed. The full scale (1/1) 3D model prepared for CFD analyses is shown in Figure 2.

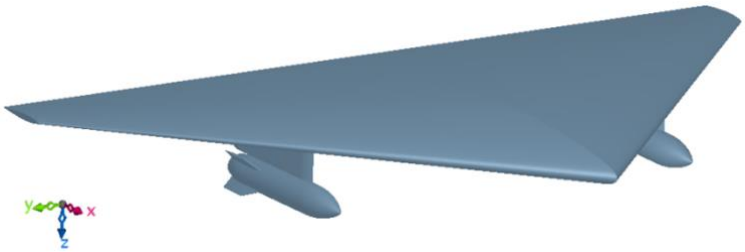

Figure 2: The 3D model of the wing/pylon/finned store constructed for CFD analyses

Angular rotation axes and angular definitions were established based on the three-view representation of the 3D CFD analysis model. The origin of the coordinate system in the 3D model is set at the center of gravity of the finned store. Rotations about the X, Y and Z axes are denoted by φ (phi), θ (theta), and ψ (psi), respectively. The orientation of the coordinate system, the angular rotation axes, and their definitions in the 3D CFD model were aligned with those used in the study by Lijewski et al. [2]. The mass and moments of inertia of the finned store are presented in Table 1. The 3D CFD analysis model along with the angular definitions is shown in Figure 3 below.

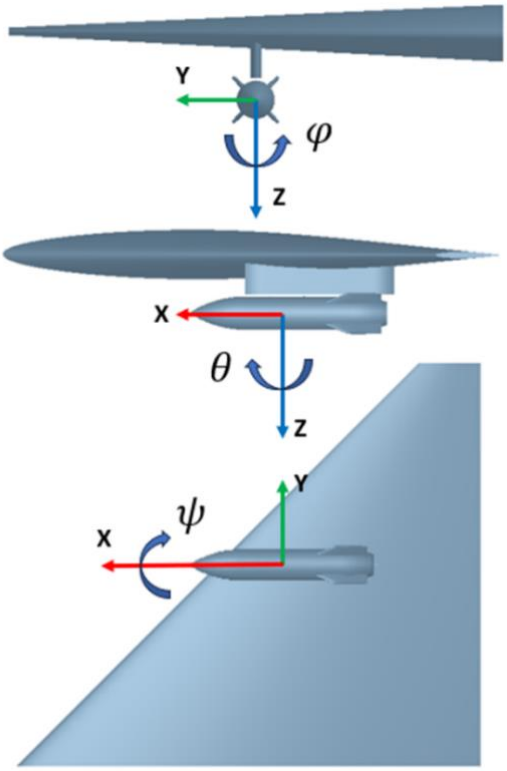

Figure 3: Angular rotation axes and angular definitions of the finned store

Table 1. Mass, center of gravity and moments of inertia data of the finned Store

Finned store mass	907.18 kg
Finned store center of gravity	X:0 m, Y:0 m, Z:0 m
Ixx	27.12 kgm^2
Iyy	488.1 kgm^2
Izz	488.1 kgm^2

2.2 Computational Domain and Boundary Conditions

The analysis was conducted using compressible air as the analysis fluid. Boundary conditions for the simulation were obtained from the study by Lijewski et al. [2]. An altitude of 26000 ft and an airspeed of Mach 0.95 were used as the boundary conditions for the analysis. At 26000 ft altitude, according to the International Standard Atmosphere (ISA), the static ambient pressure is 35.988 kPa, ambient temperature is -36.5 °C and the speed of sound is 308.6 m/s. Since there was no side slip angle and to reduce computational time, a symmetric model was employed. The computational domain is illustrated in Figure 4 below. At the inlet, a velocity boundary condition of 293.132 m/s was applied, while the outlet boundary was set to a static altitude pressure of 35.988 kPa. Free slip boundary conditions were defined for the side walls. Two ejector thrusters are installed on the pylon. These thrusters apply a constant vertical force (+Z direction) to the finned store from the initial instant up to 0.05 seconds. The forward thruster is located 1.24 m from the nose cone, while the aft thruster is positioned 1.75 m from the nose. The forward thruster exerts a force of 10675.7 N, and the aft thruster applies 42702.9 N to the finned store. The trajectory of the finned store is governed by aerodynamic forces, gravity and the ejector forces. Figure 5 shows the forces acting on the finned store.

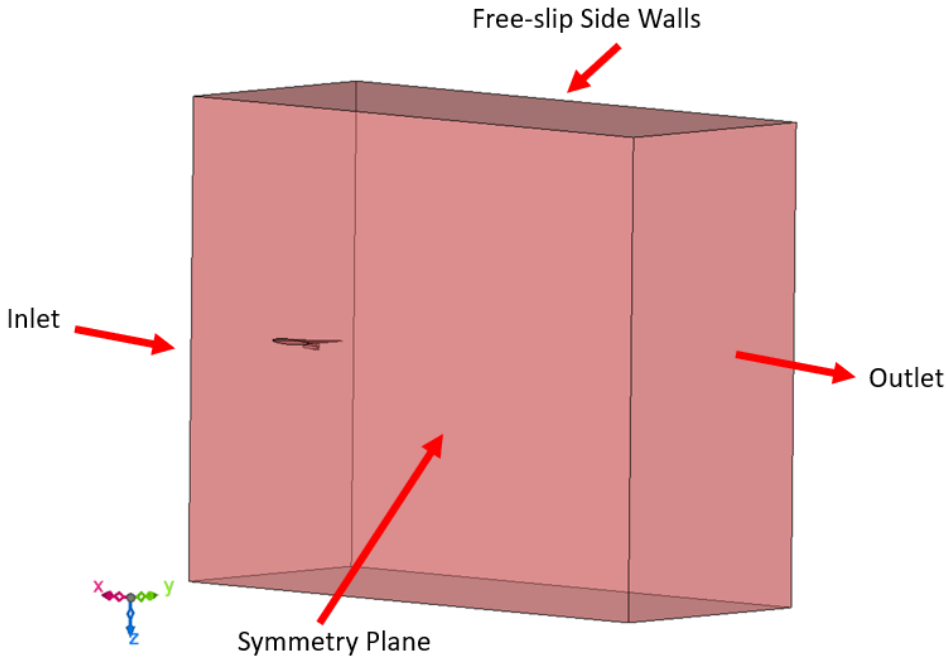

Figure 4: 3D CFD analysis symmetric computational domain model

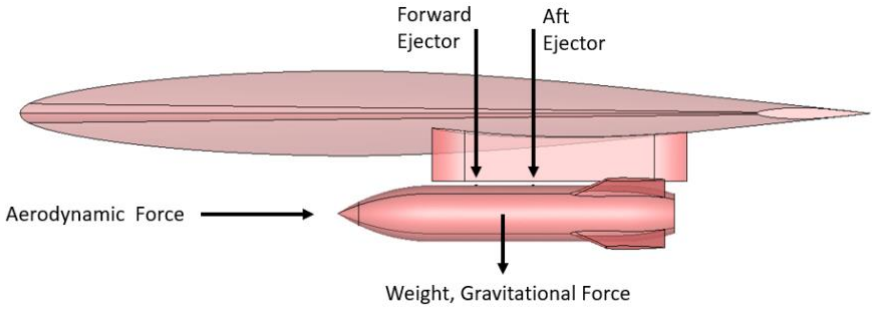

Figure 5: Forces governing the trajectory of the finned store

To calculate the trajectory of the finned store, the rigid body solver, overset mesh and moving elements features of the Cradle CFD software were enabled. A second order numerical solver was selected to enhance solution accuracy.

The turbulence model used in the analysis was the standard k-ε model. This model is well suited for turbulence calculations in free stream flow regions and offers advantages in boundary layer velocity profile computations and mesh density requirements. To improve boundary layer velocity profile predictions, the software's adaptive wall function feature was enabled. This function engages where the mesh resolution is insufficient to capture velocity gradients near walls, performing the necessary near wall velocity computations. Activating the adaptive wall function allows for a reduced mesh element count and lower computational load, thus decreasing overall solution times.

Since the analysis involved transonic speeds with compressible flow, a Density Based Solver was employed. No slip wall boundary conditions were applied on all wall surfaces of the Wing/Pylon/Finned store geometry.

The analysis was initially performed as a steady state simulation, enabling flow development and convergence around the geometry. The converged steady state flow field was then used as the initial condition for the transient analysis. The transient simulation was run for 0.35 s to compute the trajectory of the finned store. A time step of 2×10^{-6} s was selected, considering the Courant number and convergence criteria.

To monitor and record the displacement of the finned store, a total of four reference points were defined; one in front of the nose cone and three alongside the center of gravity. The coordinates of these points were recorded at intervals of 1×10^{-5} s. Trajectory calculations were performed based on the data from these reference points.

2.3 Computational Domain and Mesh Structure

The computational domain dimensions are 85 m along the X axis, 35 m along the Y axis, and 70 m along the Z axis. These dimensions were chosen to ensure that the domain boundaries exert negligible influence on the flow, using the characteristic wing root chord length as the reference dimension. Specifically, the inlet boundary is located at a distance equivalent to twice the reference length, the outlet boundary at ten times the reference length downstream, and five times the reference length in both vertical and lateral directions. The computational mesh comprises approximately 2.3 million nodes and 1.1 million elements. Figure 6 and Figure 7 below illustrate the mesh structure of the

computational domain. The general mesh element size in the domain is 1.6 m. Element sizes on the wing surface are 0.1 m, on the leading and trailing edges of the wing 0.025 m, on the pylon surface 0.05 m, on the finned store surface 0.025 m, on the fins 0.0125 m and on the fin edges 0.00625 m. A refined numerical region with an element size of 0.4 m was defined in the flow region through which the finned store trajectory region.

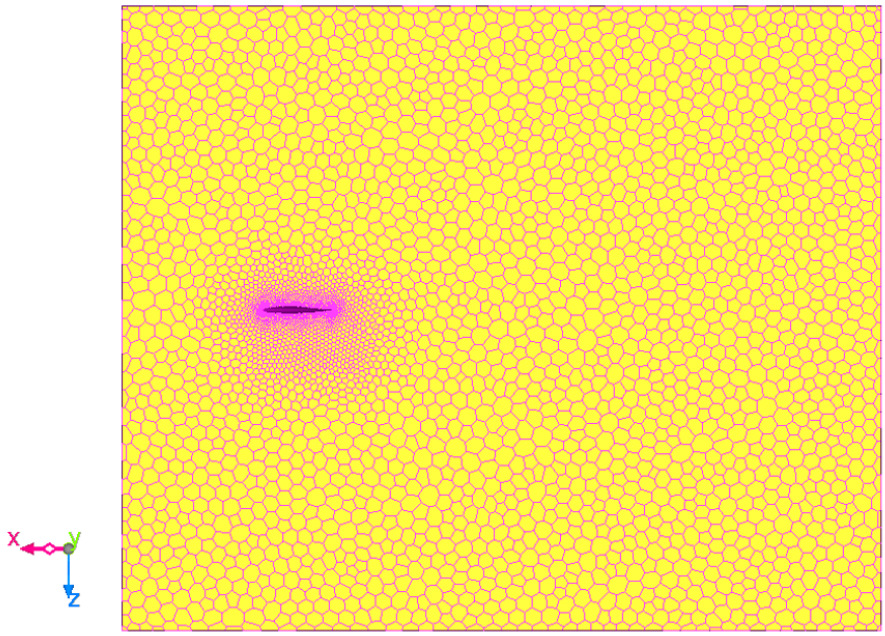

Figure 6: Computational domain mesh view

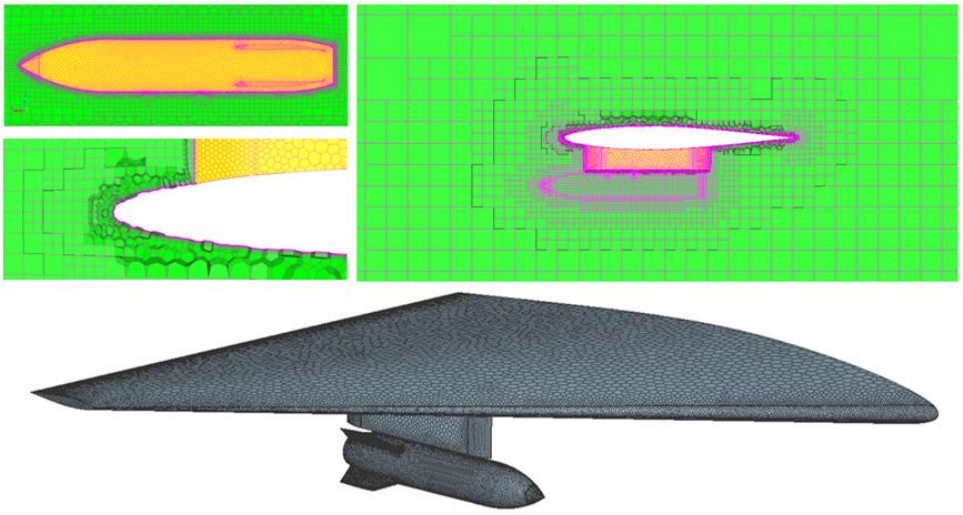

Figure 7: Computational domain mesh detail view

3. COMPUTATIONS

3.1 Conservation Equations

The CRADLE CFD software performs numerical analysis by solving the Navier-Stokes equations. These equations represent the conservation laws of mass, momentum and energy and their numerical solutions are obtained using the Finite Volume Method (FVM). In the Finite Volume Method, the overall balance between the inlet and outlet is considered within each control volume to represent a conservation equation. The continuity equation for incompressible flow is given in Equation (1). The momentum conservation equation for incompressible flow is presented in Equation (2). The energy equation for incompressible flow is provided in Equation (3) [4].

$$\frac{\partial u}{\partial x}+\frac{\partial v}{\partial y}+\frac{\partial w}{\partial z}=0 \tag{1}$$

$$\rho\left(\frac{\partial u}{\partial t}+\frac{\partial u}{\partial x}u+\frac{\partial u}{\partial y}v+\frac{\partial u}{\partial z}w\right)=-\frac{\partial p}{\partial x}+\mu\left(\frac{\partial^2 u}{\partial x^2}+\frac{\partial^2 u}{\partial y^2}+\frac{\partial^2 u}{\partial z^2}+\right)+\rho g_x \tag{2}$$

$$\frac{\partial \rho C_p T}{\partial t}+\frac{\partial u_j \rho C_p T}{\partial x_j}=\frac{\partial}{\partial x_j}K\left(\frac{\partial T}{\partial x_j}\right)+\dot{q} \tag{3}$$

$\rho : density$ $C_p : specific\ heat$ $\dot{q} : heat\ source$ $T : temperature$ $t : time$
$\mu : viscosity$ $g_x : gravity$ $u, v, w : x, y, z\ velocity\ components$
$K : thermal\ conductivity$ $u_j : velocity\ in\ the\ j-direction$

3.2 Standard k-ε Türbülans Modeli

Standard k-ε Turbulence Model

In the Standard k-ε turbulence model, the turbulence kinetic energy (k), energy dissipation rate (ε), and turbulent viscosity (μT, eddy viscosity) are calculated as follows.

$$k=\frac{\overline{u_,'u_,'}}{2} \tag{4}$$

$$\varepsilon=\nu\overline{\frac{\partial u_i'}{\partial x_j}\frac{\partial u_i'}{\partial x_j}} \tag{5}$$

$$\mu_t|k\varepsilon=C_\mu\rho\frac{k^2}{\varepsilon} \tag{6}$$

The transport, advection, diffusion, and dissipation of the k and ε parameters are computed using the following equations, which are known as the k-ε equations [4].

$$\frac{\partial \rho k}{\partial t} + \frac{\partial u_i \rho k}{\partial x_i} = \frac{\partial}{\partial x_i}\left(\frac{\mu_t}{\sigma_k}\frac{\partial k}{\partial x_i}\right) + G_S + G_T - \rho\varepsilon \quad (7)$$

$$\frac{\partial \rho \varepsilon}{\partial t} + \frac{\partial u_i \rho \varepsilon}{\partial x_i} = \frac{\partial}{\partial x_i}\left(\frac{\mu_t}{\sigma_\varepsilon}\frac{\partial \varepsilon}{\partial x_i}\right) + C_1\frac{\varepsilon}{k}(G_S + G_T)(1 + C_3 R_f) - C_2\frac{\rho\varepsilon^2}{k} \quad (8)$$

$$G_S = \mu_t\left(\frac{\partial u_i}{\partial x_j} + \frac{\partial u_j}{\partial x_i}\right) \qquad G_T = g_i\beta\frac{\mu_t}{\sigma_t}\frac{\partial T}{\partial x_i} \qquad R_f = -\frac{G_T}{G_S + G_T}$$

The model coefficients are listed in Table 2.

Table 2: Standard k–ε turbulence model coefficients

σ_k	σ_ε	σ_t	C_1	C_2	C_3	C_μ
1.0	1.3	0.9	1.44	1.92	0.0	0.9

3.3 Cradle CFD scFlow Numerical Solution

The equations presented in Sections 3.1 and 3.2 are solved iteratively within each mesh element, and the convergence criterion requires the relevant equation parameters to approach a value of at most 10^{-4} according to the literature. According to Figure 8, the numerical convergence requirements have been satisfactorily met in the analyses conducted within the scope of this study.

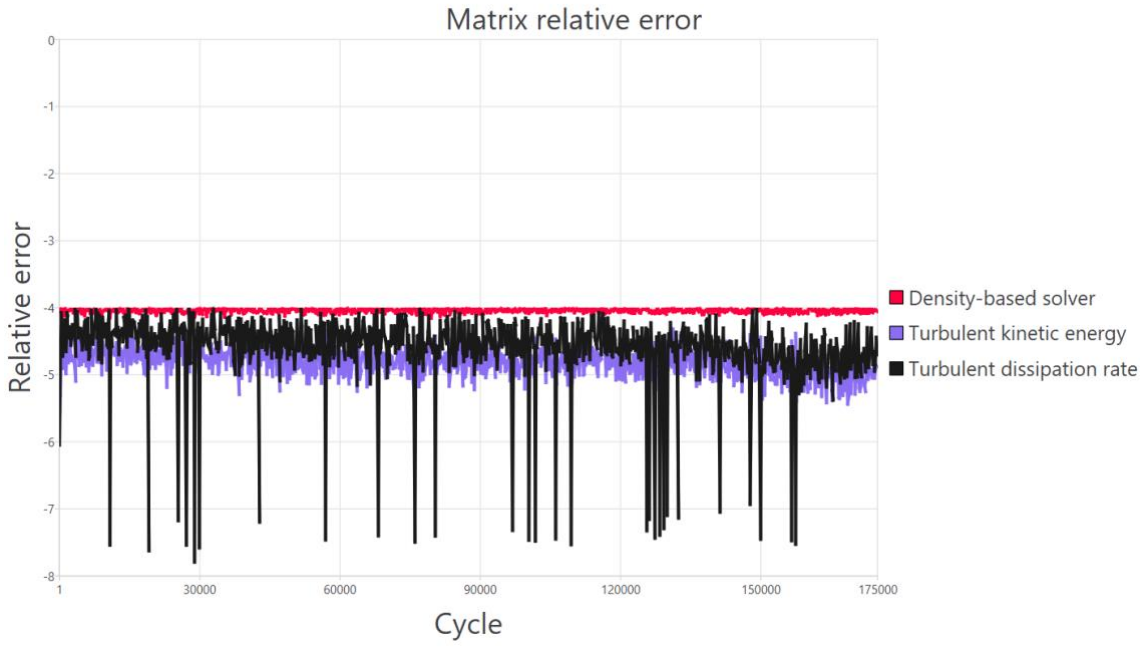

Figure 8: CFD analysis numerical convergence values

4. ANALYSIS RESULTS

As a result of the analysis, the primary objective the trajectory of the finned store was calculated. The coordinate changes of the four designated reference points were recorded at time intervals of 1×10^{-5} s. During the analysis, the displacement of these four points was monitored in real time via the Cradle CFD scSolver monitor screen. The transient variation of the coordinates of the four points is shown in Figure 9.

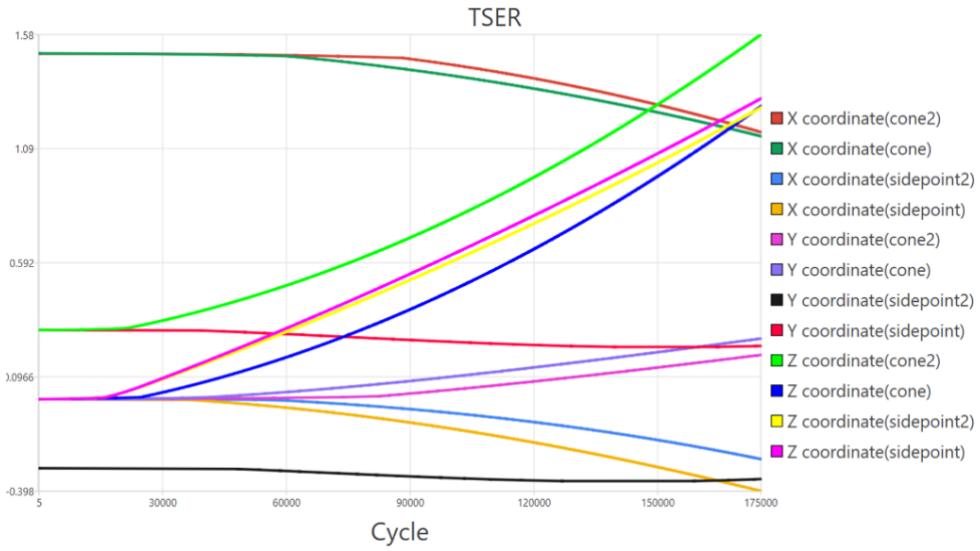

Figure 9: Transient variation of the coordinates of the four reference points

4.1 Steady State Analysis Results

Initially, a steady state analysis was conducted to allow the flow development and convergence around the wing and finned store. This analysis resulted in steady aerodynamic loads acting on the finned store. The aerodynamic forces acting on the finned store are -5522 N along the X axis, -4351 N along the Y axis, and -2507 N along the Z axis. In the analyzed delta wing configuration, the chord length and thickness increase towards the wing root. The increasing chord length and wing thickness enlarge the stagnation region and the high-pressure zone at the wing leading edge in terms of area. Similarly, the expanding chord length increases the area of the high velocity and low-pressure region generated by the wing. The pylon and finned store located beneath the wing divide the flow under the wing into two regions. There is a difference in aerodynamic flow conditions between these two regions, primarily due to the variation in the average chord length and thickness in each region. This discrepancy also influences the aerodynamic forces acting on the finned store. The pressure distribution generated by the pylon and finned store on the wing underside, wing leading edge and wing trailing edge regions is illustrated in Figure 10.

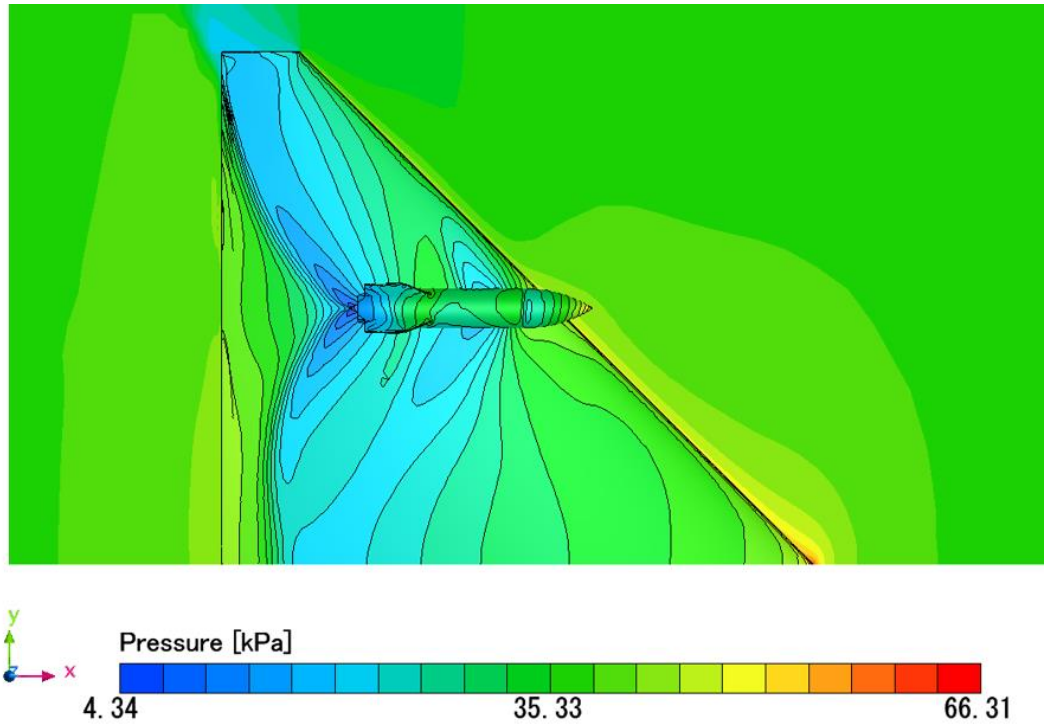

Figure 10: The effects of the pylon and finned store on the pressure distribution over the wing

Figure 11 illustrates the pressure distribution over the geometry. When these pressure values are multiplied by the unit area, they generate the pressure forces acting on the geometry. Accordingly, the finned store is subjected to high- and low-pressure regions that produce forces in the +Y direction at the conical nose section and in the -Y direction at the fin region. These pressure forces induce an angular rotation of the finned store about the positive ψ axis. The force along the X axis originates from drag. The drag force is the sum of the pressure forces and viscous friction forces generated at a flight speed of 0.95 Mach. This force tends to move the finned store in the -X direction. The wing geometry accelerates the flow and reduces pressure and similarly, the flow acceleration and pressure drop at the pylon leading and trailing edges result in generally lower pressure regions on the surfaces of the finned store facing the wing. The pressure difference on the surfaces facing the +Z and -Z directions generate the force of -2507 N along the Z axis. Since the weight of the finned store and the pylon ejector forces are much greater than the aerodynamic force in the -Z direction, the resultant force applied to the finned store is directed along the +Z axis. This condition induces a vertical displacement of the finned store.

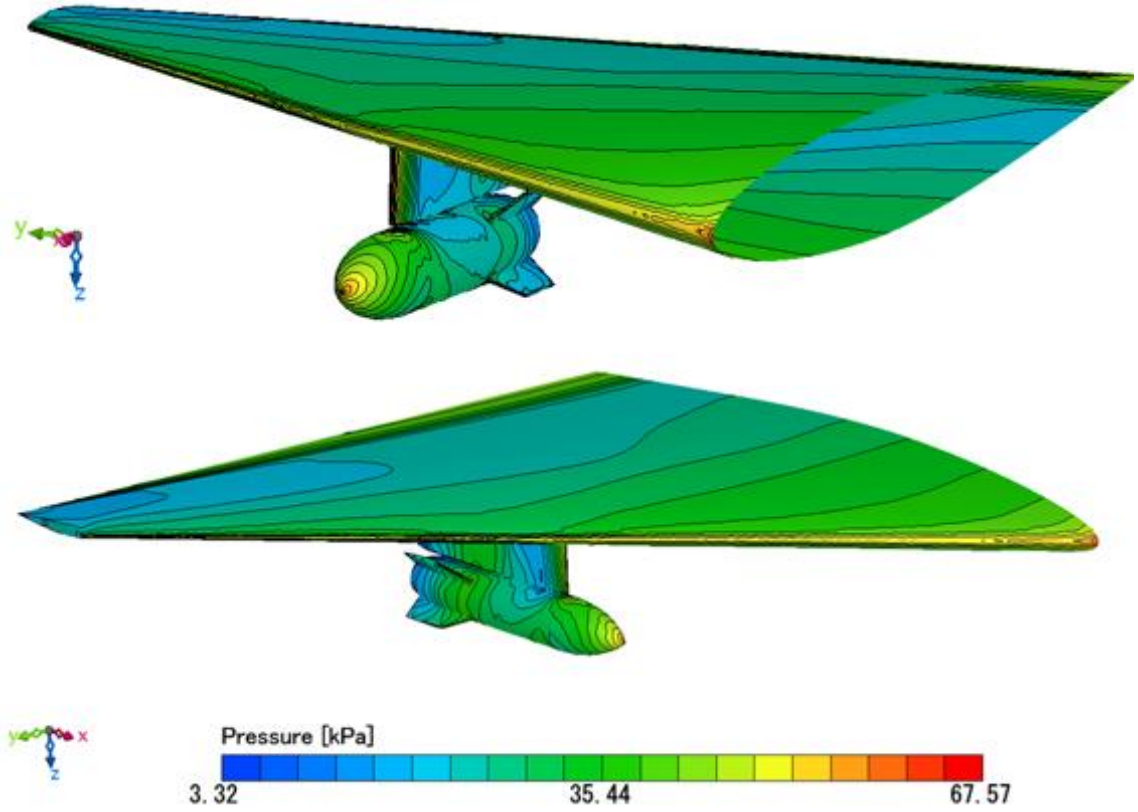

Figure 11: Pressure distribution on the wing/pylon/finned store

Examination of Figure 12 reveals the presence of a transonic flow regime around the geometry. Supersonic flow formations begin at approximately Mach 0.7 over the airfoil profile. The inlet boundary condition for the analysis is set at Mach 0.95. In regions where the wing and finned store geometries expand, the velocity increases, reaching up to approximately Mach 1.5. Transonic flow regimes pose significant challenges for CFD analyses and generally exhibit higher error margins compared to subsonic and supersonic speeds. Due to the formation of weak shock waves and rapid flow regime changes inherent to transonic conditions, achieving convergence at solution points is demanding. As an example of this challenge, Figure 13 illustrates the abrupt variation in drag coefficients within the transonic flow region from a study analyzing the drag force of an F-16 fighter jet [5].

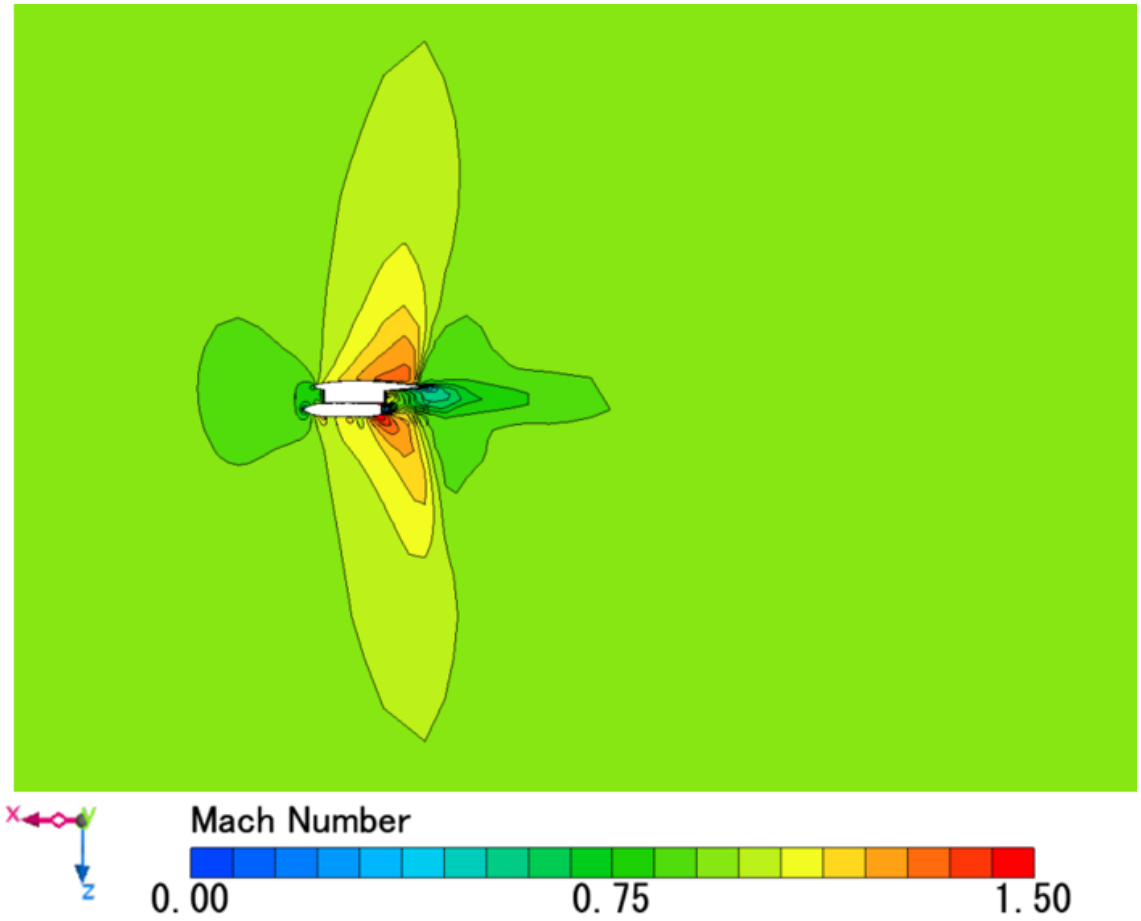

Figure 12: Mach number distribution on the plane passing through the center of the finned store

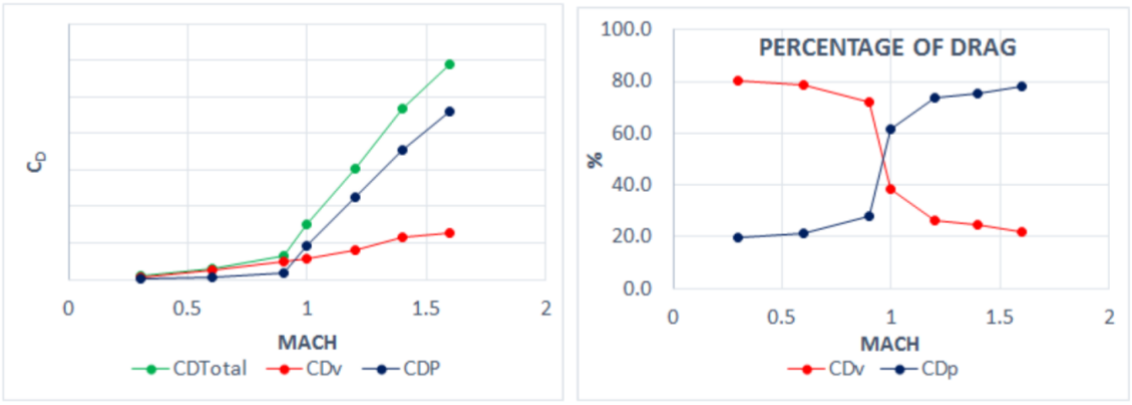

Figure 13: Variation of drag coefficients of the F16 fighter jet with Mach number

4.2 Transient Analysis Results

The trajectory calculation of the finned store was conducted through a transient analysis. The analysis was performed by utilizing the rigid body solver and the overset mesh model available in the Cradle CFD software. The total simulation duration was 0.35 s. During this period, the displacement of the finned store was recorded at the reference points along the X, Y, and Z coordinates.

Figure 14, Figure 15, and Figure 16 depict the position of the finned store at 0.12 s and 0.35 s from three different perspectives. It can be observed that during the initial motion of the finned store, the ejector forces acting on the store are dominant. The rear ejector applies a vertical force of 42712.9 N, while the front ejector applies 10675.7 N to the finned store. The center of gravity of the finned store lies between the application points of these two ejector forces. The magnitude of the rear ejector force is approximately four times that of the front ejector force. The ratio of the rear ejector force to the weight of the finned store is 4.8. The dominance of the rear ejector force is evident in the motion characteristics of the finned store. Under the influence of the rear ejector force, the finned store initially undergoes rotation about the Y axis, achieving a θ angle of 5.4° at 0.19 seconds. The rotation about the Y axis decreases over time due to aerodynamic forces and gravity, causing a nose down pitching motion. When examining the rotation about the Z axis (ψ), the moment generated by the positive pressure force on the nose region in the +Y direction and the negative pressure force on the fin region in the -Y direction results in a ψ rotation of 13.5° at 0.35 seconds. This rotation directs the nose cone of the finned store toward the wingtip. Regarding rotation about the X-axis, the pressure differential over the fins causes a φ rotation of 5.1° at 0.32 seconds.

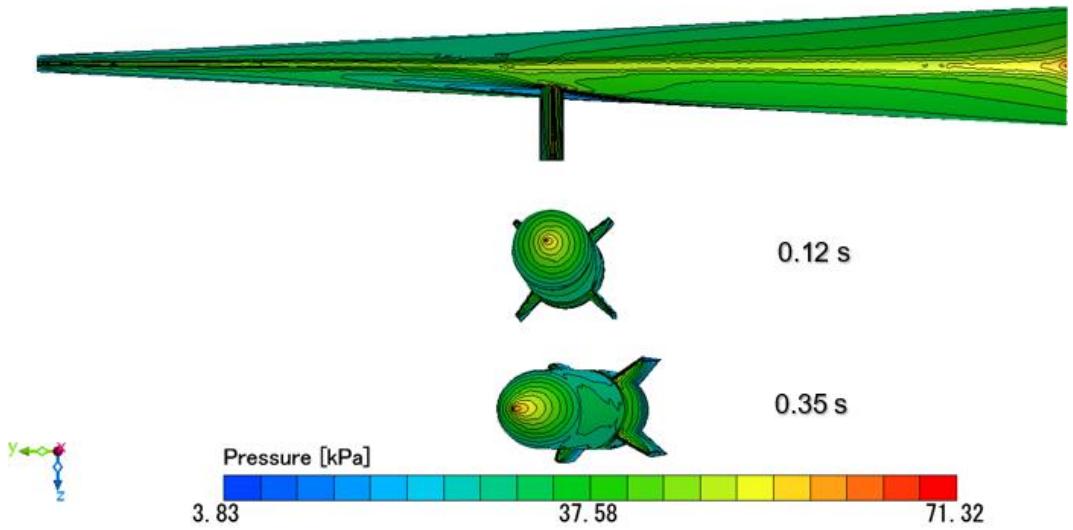

Figure 14: Position of the finned store at 0.12 s and 0.35 s (Front view)

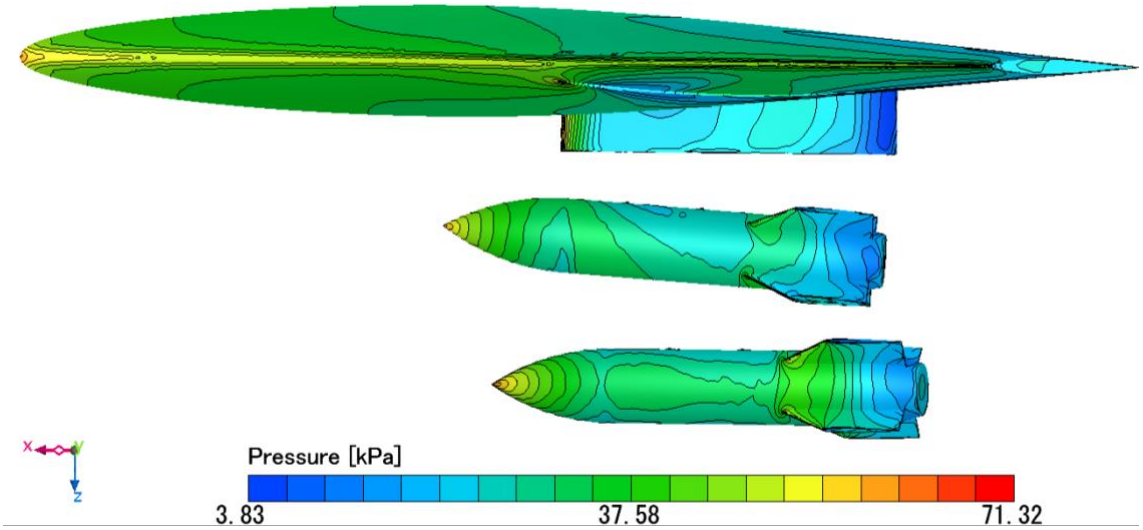

Figure 15: Position of the finned store at 0.12 s and 0.35 s (Side view)

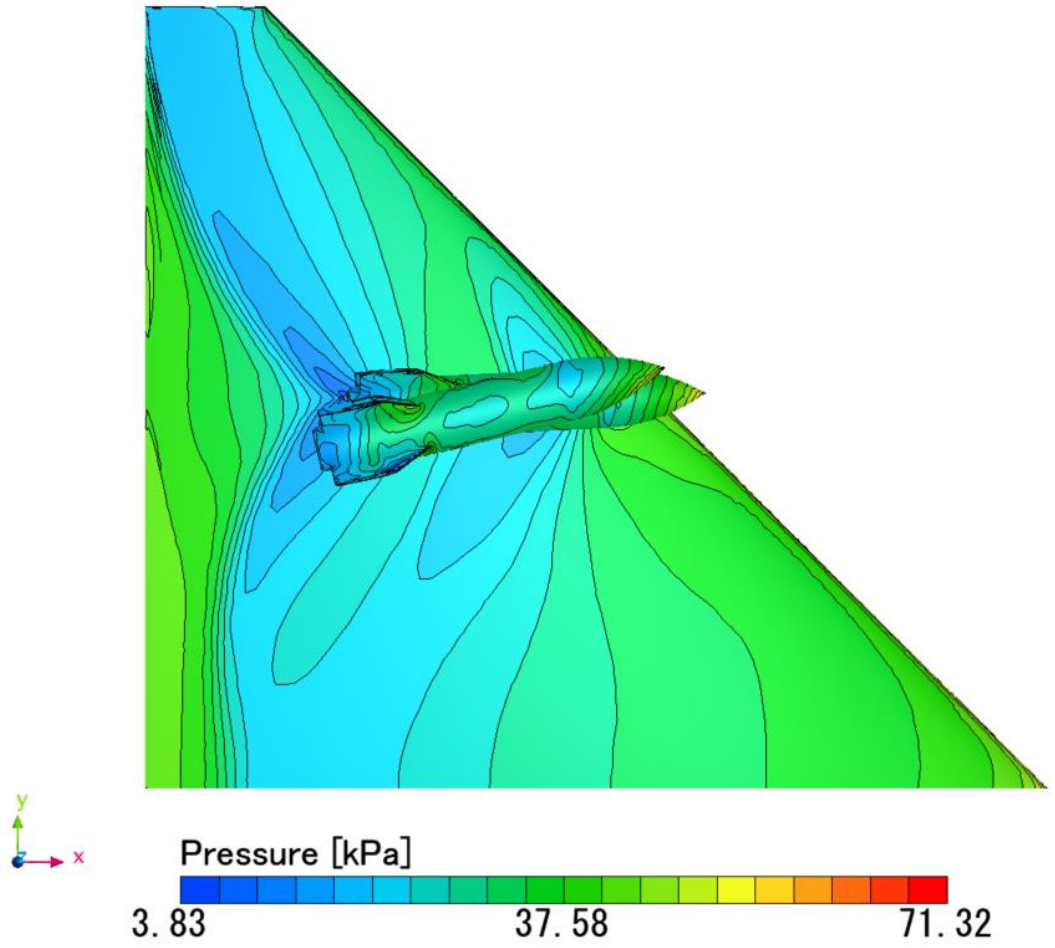

Figure 16: Position of the finned store at 0.12 s and 0.35 s (Bottom view)

The CFD analysis results obtained using the Cradle CFD software were compared with the analysis and test results reported by Lijewski et al. [2]. Figure 17 presents the variation of the finned store's center of gravity trajectory in the X, Y, and Z coordinates, Figure 18 shows the linear velocities of the center of gravity, and Figure 19 illustrates the Euler angles. Upon examining the result graphs, it is evident that the Cradle CFD simulation outcomes exhibit a high degree of correlation with the experimental data. The close agreement between the numerical trajectory calculations and test results, especially under the challenging transonic flow regime and the free flight conditions of a rigid body in air, demonstrates the computational capability and accuracy of the Cradle CFD software.

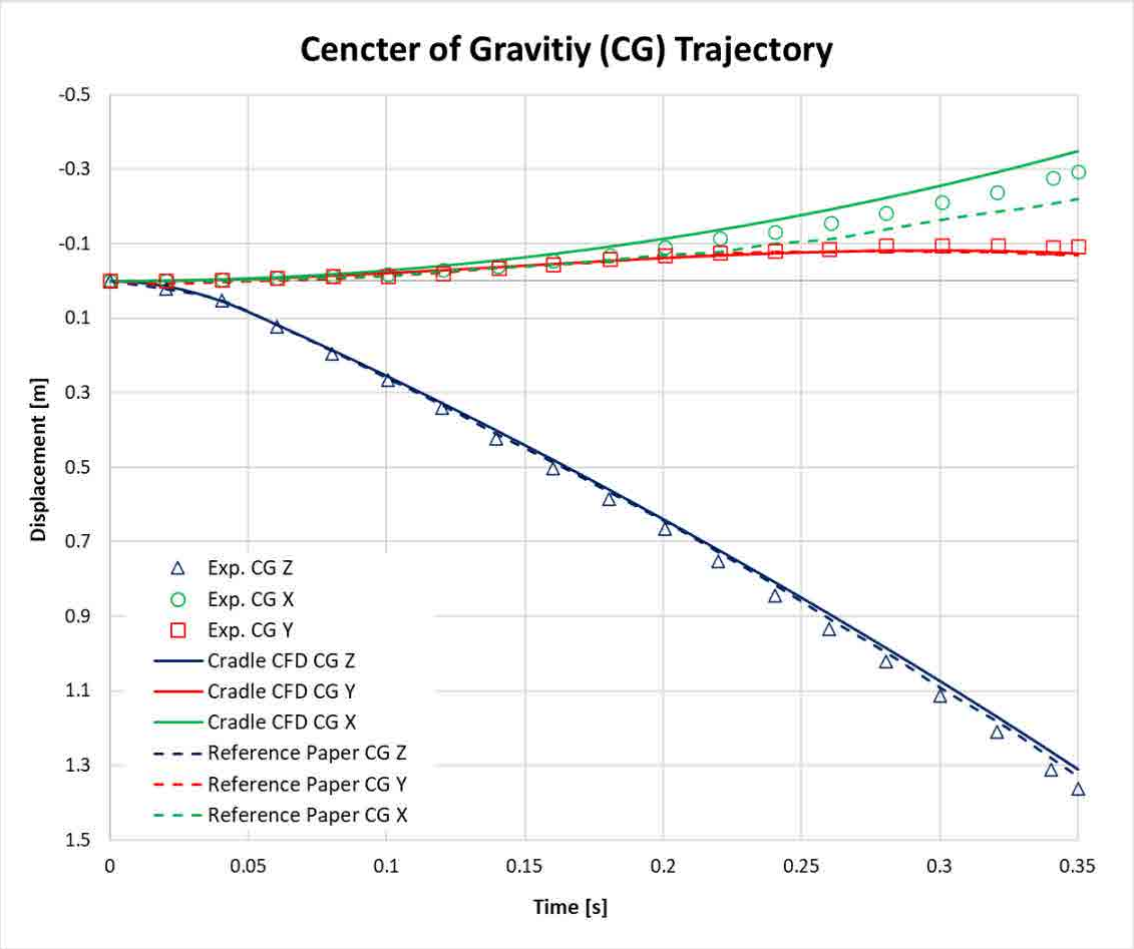

Figure 17: Displacement of the finned store's center of gravity along the X, Y, and Z axes

13.5

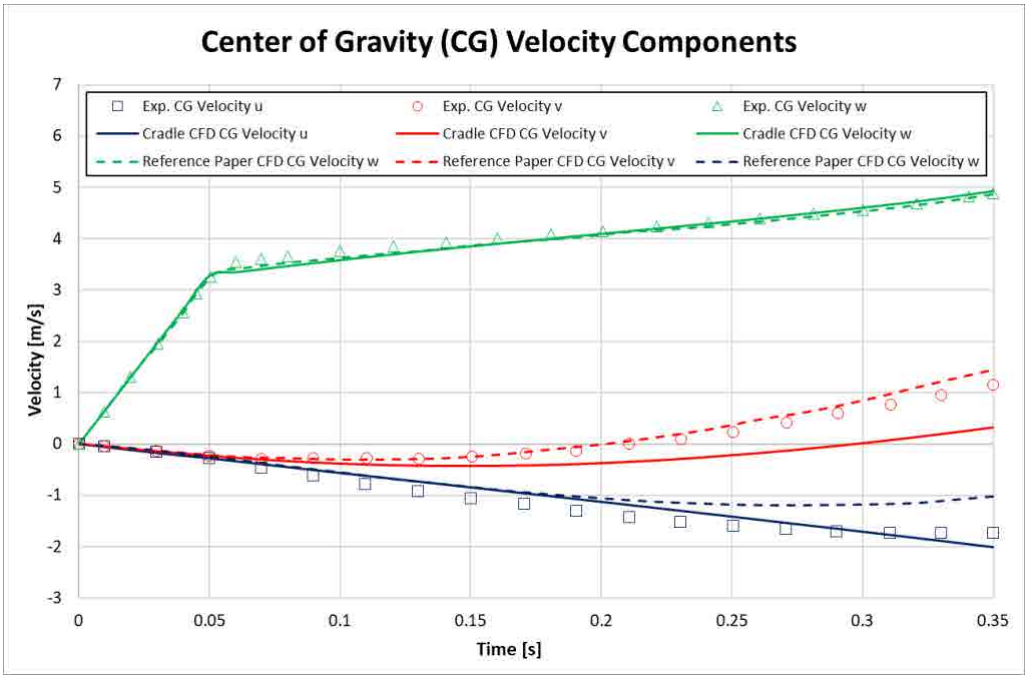

Figure 18: Velocity components of the finned store's center of gravity along the X, Y, and Z axes

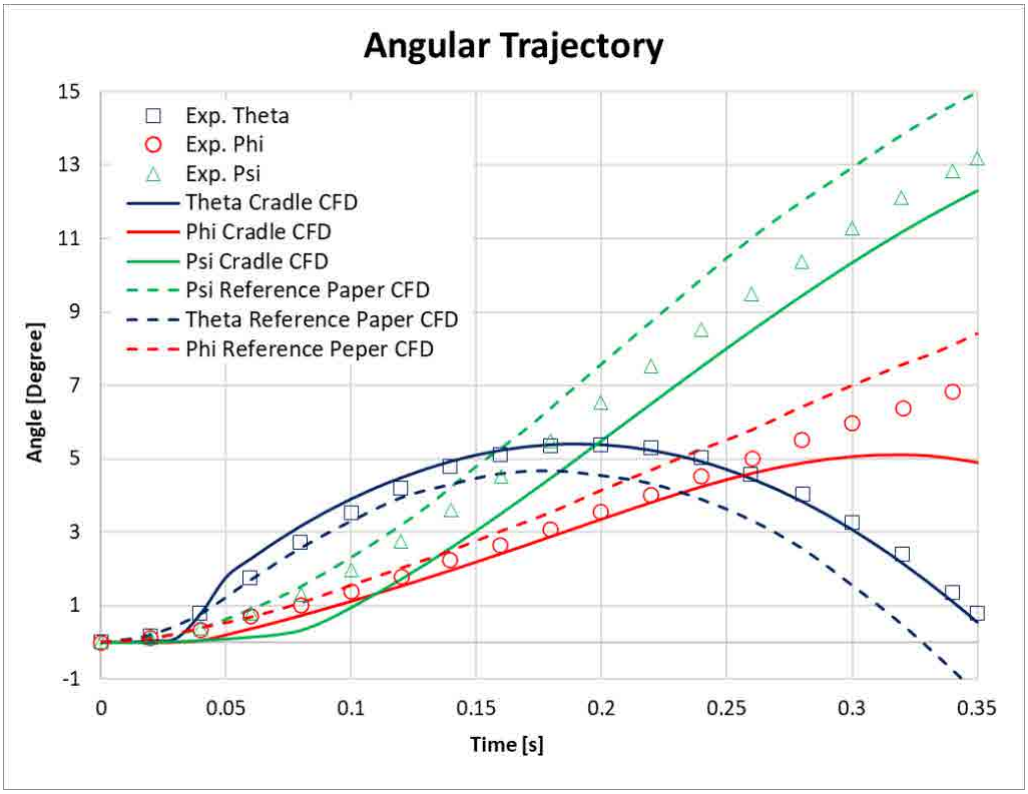

Figure 19: Angular variations of the finned store around the X, Y, and Z axes

5. CONCLUSION and DISCUSSION

In conditions dominated by transonic flow regimes, fluid variables can exhibit sudden changes. Free stream velocities close to the speed of sound may locally exceed sonic speeds around geometric obstacles or expansion regions, resulting in shock wave formation. Consequently, subsonic and supersonic flow regions coexist and interact on the geometry. This variability complicates numerical computations and can increase potential error margins.

Using Cradle CFD software, a store separation analysis was conducted under transonic flow conditions (Mach 0.95) at an altitude of 26000 ft, with a total solution time of four days. The results showed a high degree of correlation with experimental test data. Given the high cost and long test campaign schedules associated with store separation phenomena, the ability to accurately and efficiently simulate these events computationally provides significant advantages in engineering applications. Based on this validated store separation analysis, further simulations can be performed across various altitudes, speeds and geometries, enabling pre-test or pre-design validation analyses.

6 REFERENCES

[1] A. Cenko, "Experince in the use of computational aerodynamics to predict store release characteristic," *Progress inAerospace Sciences,* vol. 37, no. 5, pp. 477-495, 2001.

[2] L. E. Lijewski and N. E. Suhs, "Time-Accurate Computational Fluid Dynamics Approach to Transonic Store Separation Trajectory Prediction," *Journal Of Aircraft,* vol. 31, no. 4, 1994.

[3] H. E. Rolland, "CFD Wing/Pylon/Finned Store Mutual İnterface Winf Tunnel Experiment," Arnold Engineering Development Center, Tennessee, February 1991.

[4] *CRADLE CFD scFLOW User's Guide Analysis Method,* 2024.

[5] O. Akgun, A. I. Golcuk, D. F. Kurtulus and U. Kaynak, "Drag Analysis of a Supersonic Fighter Aircraft," in *Ninth İnternatiaonal Conference on Computational Fluid Dynamics (ICCFD9)*, İstanbul, 2016.